Effect of Lipid Molecule Headgroup Mismatch on Non Steroidal Anti-Inflammatory Drugs Induced Membrane Fusion

ARTICLE *in* LANGMUIR · DECEMBER 2011

Impact Factor: 4.46 · DOI: 10.1021/la2030186 · Source: PubMed

2 AUTHORS:

Sutapa Mondal Roy
Sardar Vallabhbhai National Institute of Tec…
11 PUBLICATIONS **90** CITATIONS
SEE PROFILE

Munna Sarkar
Saha Institute of Nuclear Physics
45 PUBLICATIONS **1,170** CITATIONS
SEE PROFILE

Langmuir

ARTICLE

pubs.acs.org/Langmuir

Effect of Lipid Molecule Headgroup Mismatch on Non Steroidal Anti-Inflammatory Drugs Induced Membrane Fusion

Sutapa Mondal Roy and Munna Sarkar*

Chemical Sciences Division, Saha Institute of Nuclear Physics, 1/AF, Bidhannagar, Kolkata-700064, India

Supporting Information

ABSTRACT: Membrane fusion is an essential process guiding many important biological events, which most commonly requires the aid of proteins and peptides as fusogenic agents. Small drug induced fusion at low drug concentration is a rare event. Only three drugs, namely, meloxicam (Mx), piroxicam (Px), and tenoxicam (Tx), belonging to the oxicam group of non steroidal anti-inflammatory drugs (NSAIDs) have been shown by us to induce membrane fusion successfully at low drug concentration.

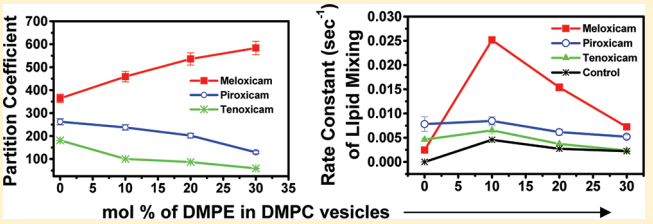

A better elucidation of the mechanism and the effect of different parameters in modulating the fusion process will allow the use of these common drugs to induce and control membrane fusion in various biochemical processes. In this study, we monitor the effect of lipid headgroup size mismatch in the bilayer on oxicam NSAIDs induced membrane fusion, by introducing dimyristoylphosphatidylethanolamine (DMPE) in dimyristoylphosphatidylcholine (DMPC) small unilamellar vesicles (SUVs). Such headgroup mismatch affects various lipid parameters which includes inhibition of trans-bilayer motion, domain formation, decrease in curvature, etc. Changes in various lipidic parameters introduce defects in the membrane bilayer and thereby modulate membrane fusion. SUVs formed by DMPC with increasing DMPE content (10, 20, and 30 mol %) were used as simple model membranes. Transmission electron microscopy (TEM) and differential scanning calorimetry (DSC) were used to characterize the DMPC-DMPE mixed vesicles. Fluorescence assays were used to probe the time dependence of lipid mixing, content mixing, and leakage and also used to determine the partitioning of the drugs in the membrane bilayer. How the inhibition of trans-bilayer motion, heterogeneous distribution of lipids, decrease in vesicle curvature, etc., arising due to headgroup mismatch affect the fusion process has been isolated and identified here. Mx amplifies these effects maximally followed by Px and Tx. This has been correlated to the enhanced partitioning of the hydrophobic Mx compared to the more hydrophilic Px and Tx in the mixed bilayer.

1. INTRODUCTION

Many processes in biological membranes occur due to the result of defects in the packing of the component molecules of the bilayer.[1] These processes include interbilayer and transbilayer lipid exchange,[2] bilayer permeation,[3] membrane fusion,[4] etc. Membrane fusion, an important event found in many biological processes, namely, neurotransmission,[5] fertilization,[6] trafficking,[7] viral infection,[8] etc., requires a significant participation of various external factors. These external factors may be in the form of other organic molecules, drugs, proteins, and peptides that induce defects and fusion in membranes. The presence of defects in the membranes, introduced by the changes in lipid parameters, can also induce and complete the fusion process.[9] The origin of such defects in a lipid bilayer can be varied, but the two common causes come from the presence of lipid molecules having different headgroup size and dissimilar fatty acyl chains.

Though small drug molecule induced membrane fusion is a rare event, non steroidal anti-inflammatory drugs (NSAIDs) induced membrane fusion, which was first shown by our group, is now a well-established phenomenon.[10−12] A direct biological consequence of this fusogenic property of one of the oxicam NSAIDs, namely, piroxicam, manifests in its ability to fuse and rupture the mitochondrial outer membrane leading to release of cytochrome c in the cytosol that signals the activation of the downstream pro-apoptotic caspase-3.[13]

Drug induced membrane fusion, unlike protein induced fusion, is controlled by the interplay of different physical and chemical parameters of both the participating drugs and the lipids. A clear understanding of that interplay will allow the use of these common drugs to induce and control membrane fusion in biotechnological and biomedical procedures where fusion forms an integral step.[14] In our previous studies,[11,12] we have already unraveled the effect of drug concentration, temperature, and low concentration of cholesterol which is known to increase the orientational order of the lipid chains. In our present study, we monitor the effect of changing the headgroup size of the lipid molecules on oxicam NSAIDs induced membrane fusion. The three drugs studied include meloxicam (Mx) [IUPAC name: (8*E*)-8-[hydroxy-[(5-methyl-1,3-thiazol-2-yl)amino] methylidene]-9-methyl-10,10-dioxo-10λ^6-thia-9-azabicyclo[4.4.0]deca-1,3,5-trien-7-one], piroxicam (Px) [IUPAC name: (8*E*)-8-[hydroxy-(pyridin-2-ylamino)methylidene]-9-methyl-10,10-dioxo-10λ^6-thia-9-azabicyclo[4.4.0]deca-1,3,5-trien-7-one], and

Received: August 3, 2011
Revised: October 12, 2011
Published: October 15, 2011

dx.doi.org/10.1021/la2030186 | *Langmuir* 2011, 27, 15054–15064

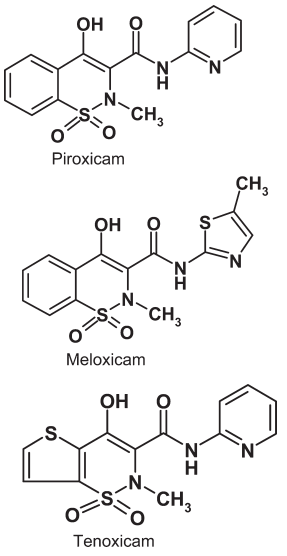

Figure 1. Chemical structures of piroxicam, meloxicam, and tenoxicam.

tenoxicam (Tx) [IUPAC name: (3*E*)-3-[hydroxy(pyridin-2-ylamino) methylene]-2-methyl-2,3-dihydro-4*H*-thieno[2,3-*e*][1,2]thiazin-4-one-1, 1-dioxide] [Figure 1].

Phosphatidylcholine (PC) and phosphatidylethanolamine (PE) are the main lipid molecules that are present in most eukaryotic cells and cell organelles.[15] PCs are the most common and most largely present phospholipid in biological membranes. They have the advantage of having neutral charge, chemical inertness, biocompatibility, and biodegradability.[16] In earlier studies, PCs and PEs derived from various natural sources were used for in vitro studies. Since natural PCs or PEs contain fatty acyl chains with a wide variety of different lengths and various degrees of unsaturation, synthetic lipid bilayer membranes are now used extensively as model membrane systems for the studies of various physiological functions.[17−20] For achieving a clear understanding of how individual parameters modulate drug induced membrane fusion, it is essential that we study their effect on simple model membrane systems. That is why the use of a synthetic lipid bilayer having only one type of fatty acyl chain will help in parsing the effect of the individual parameter, that is, the mismatch in lipid headgroup size on membrane fusion. Here we use small unilamellar vesicles (SUVs) of dimyristoylphosphatidylcholine (DMPC) mixed with 10, 20, or 30 mol % dimyristoylphosphatidylethanolamine (DMPE) to introduce an increase in headgroup size mismatch. The working temperature was chosen to be 39 °C which is close to the physiological temperature, and also at this temperature the mixed bilayers are on the whole in the sol (L_α) phase as shown by Silvius.[21] The only difference between the DMPC and DMPE headgroup is that the DMPC contains a bulky quaternary amine with three methyl substituents whereas DMPE has a primary amine headgroup containing three hydrogen substituents [Figure 2]. Since DMPE is small in size and has hydrogen atoms attached, it has the ability to interact strongly with the neighboring lipid molecules through inter- and intramolecular H-bonding.[22] This creates a close packing of the lipid bilayer with an aligned hydrocarbon tail region which decreases the area per lipid molecule.[23] The distribution of DMPE in DMPC-DMPE mixed vesicles at neutral pH is preferably concentrated in the outer monolayer of the SUVs for low concentration of DMPE content,

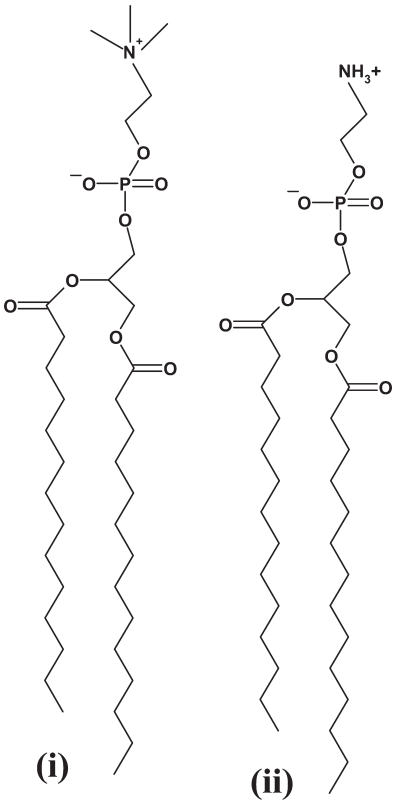

Figure 2. Chemical structures of DMPC (i) and DMPE (ii).

that is, up to 20 mol %. The distribution of DMPE in the inner monolayer of the SUVs increases above this concentration.[24] This heterogeneous distribution of PE lipids in PC-PE mixed SUVs does not show any aggregation of PE in the fluid state.[22,25] However, in the partially melted DMPE and DMPC lipid mixtures, coexistence of the gel and fluid domains occur which melt at different temperatures leading to a broadening of the gel−fluid phase transition.[26] Incomplete miscibility of both the lipids has been observed in the gel-phase according to the phase diagram as depicted earlier by Silvius.[21] In supported mixed bilayers of DMPC and DMPE, increasing temperatures resulted in the melting of the upper and the lower leaflet at different temperatures.[15] In addition, presence of 10−30 mol % DMPE in DMPC bilayers results in a significant decrease in the rate of the DMPC trans-bilayer movement, that is, flip-flop motion, considering the fact that addition of new lipid molecules to the already closely packed inner monolayer is becoming more and more difficult.[1] This has been attributed to the modulation of the spontaneous fluctuation defects in the DMPC bilayer by the presence of DMPE, which makes them more ordered. Due to such a broad spectrum of typical physical and structural properties of the mixed bilayer in the presence of DMPE within DMPC vesicles, the DMPC-DMPE mixed bilayers and vesicles are the subject of intense study for the past few decades.[27−30]

To monitor the effect of change in different lipid parameters, which arise due to headgroup mismatch, on NSAIDs induced fusion, the three major events in the fusion process, namely, lipid mixing, content mixing, and leakage, were followed. This was done by recording the time courses from the three different fluorescence assays. Content mixing and leakage were monitored

by the Tb^{3+}/DPA assay, whereas lipid mixing was monitored using the standard N-NBD-PE/N-Rh-PE assay at physiological pH 7.4. Kinetic parameters were extracted from the time courses, where the change in fluorescence intensity of the probes used in the three different assays were plotted against time. The effect of change in headgroup size was also monitored by determining the partition coefficient with increasing DMPE in DMPC SUVs. DSC was used to monitor the change in chain melting temperature in the presence of the three drugs with increasing mole concentration of DMPE. Transmission electron microscopy (TEM) images were obtained to evaluate the change in average diameter of the vesicles in the presence of enhanced concentrations of DMPE in DMPC vesicles. This detailed study will give a clear understanding of the effect of headgroup size mismatch that in turn affects several lipidic parameters, on oxicam drugs induced membrane fusion, and will help us in better elucidation of the molecular mechanism of this fusion process.

2. MATERIALS AND METHODS

Dimyristoylphosphatidylcholine (DMPC), dimyristoylphosphatidylethanolamine (DMPE), dipicolinic acid (DPA), TritonX-100 (ultrapure), Terbium (Tb^{3+}) chloride, (3-[*N*-morpholino]propanesulfonic acid) sodium salt (MOPS buffer), piroxicam, and tenoxicam were purchased from Sigma-Aldrich, meloxicam from LKT Laboratories, *N*-(7-nitrobenz-2-oxa-1,3-diazol-4-yl)-1,2-dihexadecanoyl-*sn*-glycero-3-phosphoethanolamine, triammonium salt (N-NBD-PE) and lissamine rhodamine B-1,2-dihexadecanoyl-*sn*-glycero-3-phosphanolamine, triethylammonuim salt (N-Rh-PE) from Invitrogen Life Science Corporation, and 2-[tris (hydroxymethyl) methylamine]-1-ethanesulfonic acid (TES buffer) and sodium ethylene diamine tetra aceate (EDTA sodium salt) from SRL (India), and all were used without further purification. Sephadex G-50, for size exclusion column chromatography, was purchased from Amersham Biosciences. Water was quartz distilled thrice before use. Stock solutions of meloxicam, piroxicam, and tenoxicam were prepared in dimethyl sulfoxide (DMSO) (Merck, Germany), and the exact concentration was adjusted by the corresponding buffer. The dilution of the drugs was done in such a way so that each sample contains 0.5% (v/v) DMSO, which had no significant effect over the SUV structure or membrane fusion process.[6]

2.1. Preparation of SUVs. SUVs of lipids, namely, DMPC and different mol % of DMPE (10 mol %, 20 mol % and 30 mol %), were prepared using the sonication method[31] as done in our earlier experiments. The phospholipids were dissolved in 2:1 (v/v) chloroform/methanol solution, and the solvent was evaporated to dryness under a stream of argon. The lipid film thus produced was then kept overnight inside a vacuum desiccator at −20 °C. The dried films were hydrated and swelled in buffer at pH 7.4. The composition of the buffer solution varies in accordance with the requirement of the assay. For lipid mixing assay, either N-NBD-PE and N-Rh-PE containing vesicles or probe free vesicles were prepared in 10 mM TES containing 100 mM NaCl and 0.1 mM EDTA. For content mixing assay, 10 mM TES buffer was used for DPA (80 mM) containing vesicles, and 10 mM TES buffer along with 60 mM NaCl was used for $TbCl_3$ (8 mM) containing vesicles. For leakage assay, vesicles were prepared with coencapsulated probes having 10 mM TES buffer. After hydration, the mixture was vortexed to disperse the lipids. The dispersion was then sonicated for about 10 min, in three equal time intervals, using a dr. Heilscher (Germany) probe sonicator (200 W). The samples were then allowed to stand for 40 min at 39 °C to be hydrated completely. The sonicated samples were then centrifuged at 10 000 rpm for 15 min to remove titanium particles and aggregated lipids. These titanium particles were introduced as an impurity from the sonicator probe during process of sonication.[32]

2.2. Estimation of Phosphate. The phospholipid concentration was measured following the published protocol[33] already used in our previous experiments. Vesicle samples of 0.2 mL were digested with 0.8 mL of perchloric acid at 180 °C for 3 h. After cooling to room temperature, 5.0 mL of distilled water was added to it. Then 0.5 mL of 5% ammonium molybdate solution was added followed by addition of 0.4 mL of amminonaphthol sulfonic acid (ANSA) reagent (prepared by dissolving 7.5 g of sodium metabisulfate, 0.5 g of sodium sulfite, and 0.125 g of ANSA in 50 mL of distilled water). The solutions were allowed to stand for 20 min to develop the blue color. The amount of phosphate was estimated from the absorbance measured at 660 nm using a JASCO V − 650 absorption spectrophotometer. The lipid concentration (DMPC together with DMPE) in all the experiments was around 1.0 mM as determined by this method (data not shown).

2.3. Transmission Electron Microscopy (TEM) Measurement. TEM experiments were done with a FEI electron microscope model Tecnai G2 20S Twin operating at 200 KV with a resolution of 0.2 nm. Samples were spread over a copper grid coated with carbon. SUVs were negatively stained with 2% (v/v) phosphotungstic acid (PTA). The samples were spread over the copper grid and kept for around 2 min, and then they were dried. The PTA solution was then spread over the copper grid containing dehydrated lipid samples. The PTA solution was kept only for 20 s over the dehydrated samples so that, apart from staining, no significant morphological and size change occurred to the dehydrated lipid vesicles. The stained samples on the copper grid were further dried in a vacuum desiccator for about 3 days. The magnifications were at 19 500× for different samples, which are mentioned on the transmission electron micrographs. SUVs of DMPC and DMPC containing 10, 20, and 30 mol % DMPE were used in the experiments to compare the sizes of the vesicles on addition of the DMPE in DMPC SUVs without the presence any drug.

The frequency of distribution plots of the average diameter of the vesicles were calculated from the TEM slides. For each sample under consideration, data from at least four slides were taken. For each TEM slide, the diameters of the vesicles were obtained using the software ImageJ 1.44p, National Institute of Health, USA. The data thus obtained were used to make a calculation of the frequency of distribution, and finally it was plotted as a histogram where the *y* axis is the product of number frequency *f* and *x* where *x* is the midpoint of the interval chosen against the average diameter of the vesicles. For such grouped data, the mean diameter is given by $\Sigma fx/\Sigma f$.

2.4. Differential Scanning Calorimetry (DSC). For the DSC experiments, 1 mM lipid (DMPC + 10, 20, or 30 mol % DMPE) films were prepared, following similar method as described in the "Preparation of SUVs" section. The dried lipid films were hydrated in 10 mM MOPS buffer at pH 7.4. Constant concentration of 30 μM of the oxicam NSAIDs was also used. The DSC scans were taken 2 h after drug addition to ensure the completion of the fusion event in the presence of drugs. The DSC measurements were done using a Microcal, LLC (Northampton, MA) VP-DSC Micro calorimeter. All the samples and the buffer were degassed by spinning them in the Eppendorf centrifuge (5415D) at 13 000 rpm for 30 min and loading them into the sample and reference cells, respectively. Every sample was scanned four to five times from 5 to 60 °C with a scan rate of 20 °C/h. In all cases, the last two scans were identical. The DSC curves were analyzed by using the fitting program Origin 7.0, provided by Origin Lab (Northampton, MA).

2.5. Calculation of Partition Coefficient (K_P). The partition coefficient (K_P) of the oxicam drugs, namely, Mx, Px, and Tx, between the aqueous phase, that is, the buffer phase at pH 7.4, and the lipid phase, that is, the DMPC vesicles along with varying concentration of DMPE (10, 20, and 30 mol %) was estimated. The change in fluorescence intensity of the drugs in both the phases was monitored, and from there the partition coefficient value is calculated. All emission spectra were

corrected for instrument response at each wavelength. A 2 mm × 10 mm path length quartz cell was used for fluorescence measurements to avoid any blue edge distortion of the emission spectrum due to the inner filter effect.

At pH 7.4, all three oxicam NSAIDs exist in their anionic form.[34] The absorption maxima of the anionic forms of Mx, Px, and Tx in a hydrophobic environment are at 362, 363, and 368 nm, respectively, and the emission maximum of Mx, Px, and Tx is at 500 nm.[32,35] For the calculation of the partition coefficient values, the changes in the fluorescence intensity of the respective drugs at λ_{em} = 500 nm were monitored using a Hitachi F-4010 fluorescence spectrophotometer, with increasing concentration of lipid (DMPC containing DMPE). The respective plots are hyperbolic in nature, which indicates a noncooperative partitioning of the drugs in the lipid vesicles.

From the fluorescence emission spectra, the partition coefficients (K_P) of the three oxicam drugs were calculated using the following equation.[36]

$$I = \frac{I_W + K_P \gamma I_{max}[L]}{1 + K_P \gamma [L]} \quad (1)$$

where I = fluorescence intensity of the drugs, that is, Mx, Px, and Tx, at any concentration of lipid; I_W = fluorescence intensity of the drugs, that is, Mx, Px, and Tx, in aqueous phase, that is, buffer phase; I_{max} = maximum fluorescence intensity of the oxicam drugs at saturating lipid concentration; K_P = partition coefficient of the oxicam drugs between lipid phase and aqueous phase; γ = molar volume of lipid; and [L] = concentration of lipid added during titration. Nonlinear least-squares fitting of the I versus [L] plot was done using eq 1. The value of γ was considered as 0.95.[37] Maximum fluorescence intensity I_{max} was obtained using the following equation.[38]

$$\frac{1}{\Delta I} = \frac{1}{\Delta I_{max}} + \frac{1}{K_{app}\Delta I_{max}} \times \frac{1}{[\text{lipid}] - [\text{drug}]} \quad (2)$$

where ΔI = the change in fluorescence intensity at any concentration of lipid, ΔI_{max} = the maximum change in fluorescence intensity at the saturating molar concentration of lipid, and K_{app} = the apparent partition coefficient of the drug between the lipid and aqueous phase.

Since the concentration of the drugs, that is [drug] is almost negligible compared to the concentration of the lipid added, that is, [lipid], hence during the calculation of partition coefficient values, [drug] was considered negligible. A plot of $1/\Delta I$ versus $1/$[lipid] gave a straight line with correlation coefficient greater than 0.9, whose intercept on the y-axis gives the value of $1/\Delta I_{max}$. Knowing ΔI_{max}, I_{max} can be calculated by subtracting the value of the initial fluorescence intensity from the ΔI_{max}. Finally, for the actual calculation of the value of K_P, this value of I_{max} is used in eq 1.

2.6. Lipid Mixing Assay. Measurement of the rate constant of lipid mixing was done using standard lipid mixing assay as described in previous works.[39,40] Förster resonance energy transfer (FRET) between donor and acceptor is the main basis of this assay. Two sets of vesicles, one probe containing vesicles and the other probe free vesicles, were prepared. Both of the FRET probes N-NBD-PE (donor) and N-Rh-PE (acceptor) were used at a concentration of 0.8 mol % each, in the probe containing vesicles. Both sets of vesicles were prepared in 10 mM TES, 100 mM NaCl, and 0.1 mM EDTA buffer at pH 7.4. The probe containing vesicles were mixed with probe free vesicles at a ratio of 1:9 for the measurement. As membrane fusion occurs due to the presence of drugs, lipids of probe containing vesicles get mixed with the lipids of the probe free vesicles, resulting in dilution of the probes on the fused vesicles. Thus, membrane fusion decreases the FRET due to enhanced probe distances which resulted in fluorescence dequenching of N-NBD-PE. This increase in fluorescence intensity was monitored with time using a HORIBA Jobin Yvon Fluoromax-3 fluorescence spectrophotometer with an excitation at 460 nm and emission at 530 nm. The fluorescence data were taken at a constant concentration of the oxicam NSAIDs at 30 μM, that is, drug to lipid (D/L) ratio at 0.03 and at constant temperature of 39 °C. As already mentioned in the earlier work,[7] oxicam drugs have a significant amount of quenching effect on the fluorescence intensity of the lipid probes. This quenching effect was calculated and nullified from the original time course as was done in our previous work.

The lipid mixing is given by the following equation:

$$\%\ \text{lipid mixing} = \frac{F - F_0}{F_\infty - F_0} \times 100 \quad (3)$$

where F = fluorescence intensity at time t, F_0 = initial fluorescence of the labeled liposomes set as 0% fluorescence, and F_∞ = the maximum fluorescence set as 100%; it was determined by lysing the vesicles with 1% (v/v) Triton X-100, thereby releasing the probes in aqueous buffer resulting in high dilution and total absence of FRET. We used ultrapure Triton X-100, which did not affect the N-NBD-PE fluorescence, and hence, the correction factor of 1.4−1.5 was not used.[40]

Each lipid mixing experiment is repeated at least three to four times, and the error bars in the data points represent the standard deviation of that data point. All the time courses of lipid mixing could be fitted to a single exponential rate equation: $f = a(1 - \exp(-kt))$ where the exponential constant k is referred to as the rate constant and the extent of percentage of lipid mixing at infinite time is given by the pre-exponential factor a.

2.7. Content Mixing Assay. The rate constant of content mixing of the inner contents of the fusing vesicles was measured using the standard Tb-DPA assay.[12,41] Two sets of vesicles were prepared, one encapsulated with DPA (80 mM) and the other encapsulated with $TbCl_3$ (8 mM) in the specific buffer as already discussed earlier in section 2.1 at pH 7.4. The untrapped probes, present in the external buffer of the vesicles, were removed using a Sephadex G-50 column equilibrated with the elution buffer (10 mM TES, 100 mM NaCl, 1 mM EDTA at pH 7.4). To define the 0−100% interval, $TbCl_3$ containing vesicles were also rechromatographed in the absence of EDTA. This was lysed with Triton X-100 at 1% (v/v), and the fluorescence intensity was recorded both in the absence and in the presence of an excess amount of DPA. Membrane fusion was monitored in the presence of various concentration of DMPE (10, 20, and 30 mol %) in DMPC vesicles induced by constant concentration of oxicam NSAIDs of 30 μM, that is, D/L ratio of 0.03 at 39 °C.

During the determination of drug induced content mixing, 30 μM of oxicam NSAIDs solutions was added to a (1:1) mixture of Tb^{3+} and DPA-containing vesicles. As fusion occurs, a highly fluorescent Tb-DPA complex is formed inside the fused vesicles. The complex fluoresces at 490 nm upon being excited at 275 nm. The content mixing was monitored in terms of an increase in fluorescence intensity at 490 nm with time using a HORIBA Jobin Yvon Fluoromax-3 fluorescence spectrophotometer. From the time courses of the content mixing, the percent of content mixing was calculated using the following equation:

$$\%\ \text{content mixing} = \frac{(F - F_0)/F_0}{(F^l - F_0^l)/F_0^l} \times 100 \quad (4)$$

where F = fluorescence intensity of Tb-DPA complex at time t, F_0 = fluorescence intensity of Tb-DPA complex at t = 0, F^l = fluorescence intensity of rechromatographed, lysed Tb-vesicles in presence of adequate amount of DPA, and F_0^l = fluorescence intensity of rechromatographed, lysed Tb-vesicles in absence of DPA

The content mixing experiments were also repeated three to four times, and the standard deviation is included as the error bars in the data. Similar to the time courses of the lipid mixing assay, all the time courses of content mixing were fitted to a single exponential rate

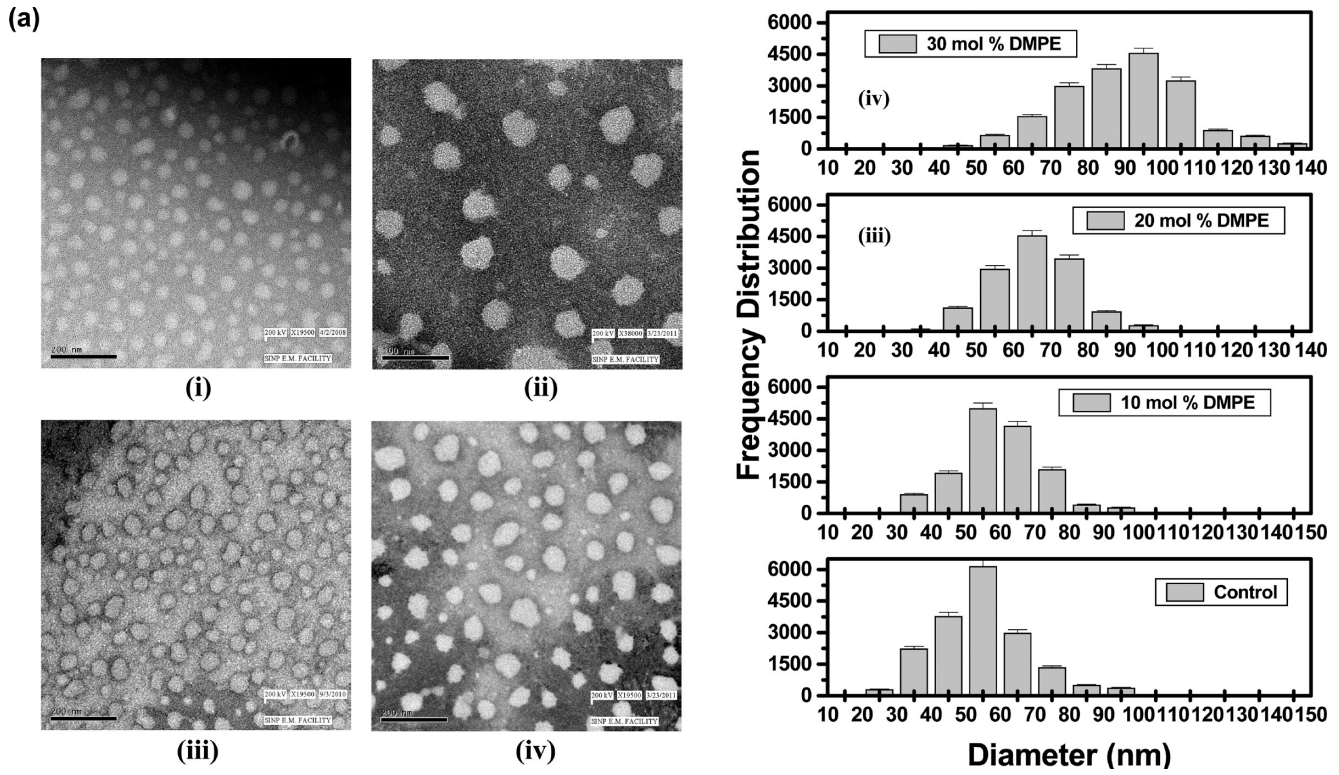

Figure 3. (a) Transmission electron microscopy images of untreated DMPC vesicles (control) (i), untreated DMPC vesicles containing 10 mol % DMPE (ii), 20 mol % DMPE (iii), and 30 mol % DMPE (iv). In all cases, grids were prepared just after vesicle preparation and stained with phosphotungstic acid (PTA). (b) Frequency distribution with respect to diameter of DMPC vesicles (i), DMPC vesicles containing 10 mol % DMPE (ii), 20 mol % DMPE (iii), and 30 mol % DMPE (iv) without any treatment with oxicam NSAIDs at 37 °C and pH 7.4, calculated from TEM micrographs. For calculation, at least four micrographs of each sample were used.

equation: $f = a(1 - \exp(-kt))$, where the exponential constant k is referred to as the rate constant and the extent of percentage of content mixing at infinite time is given by the pre-exponential factor a.

2.8. Leakage Assay. The leakage assay was performed by using coencapsulated Tb-DPA vesicles, already referred in our previous papers.[12,39] Tb^{3+} (8 mM) and DPA (80 mM) coencapsulated DMPC vesicles with varying concentration of DMPE (10, 20, and 30 mol %) were prepared in 10 mM TES buffer at pH 7.4 and were chromatographed on a Sephadex G-50 column equilibrated with elution buffer containing EDTA at pH 7.4 to eliminate unbound $TbCl_3$ present in the external buffer. As leakage occurs in the presence of drugs, the Tb-DPA complex comes out of the vesicles and the stronger chelator EDTA competes with DPA to form the more stable Tb-EDTA complex dissociating the Tb-DPA complex. The associated decrease in fluorescence intensity was measured at 490 nm with excitation wavelength at 275 nm with time using a HORIBA Jobin Yvon Fluoromax-3 fluorescence spectrophotometer at 39 °C. The percentage leakage was calculated as

$$\% \text{ leakage} = \frac{(F_{CO}^{d,t=0} - F_{CO}^{d,det}) - (F_{CO}^{d,t} - F_{CO}^{d,det})}{F_{CO}^{d,t=0} - F_{CO}^{d,det}} \times 100 \qquad (5)$$

where $F_{CO}^{d,t=0}$ = fluorescence intensity of Tb-DPA coencapsulated vesicles at the time $t = 0$, $F_{CO}^{d,t}$ = Fluorescence intensity of Tb-DPA coencapsulated vesicles at time 't', $F_{CO}^{d,det}$ = fluorescence intensity of Tb-DPA coencapsulated vesicles after lysing with 0.1% (v/v) Triton X-100.

All the time courses of the leakage assay thus obtained were also fitted to a single exponential rate equation: $f = a(1 - \exp(-kt))$, where k measured the rate constant of leakage and pre-exponential factor a measured the extent of the leakage of contents.

3. RESULTS

Characterization of DMPC-DMPE Mixed Vesicles: TEM Imaging and DSC Thermograms. Figure 3a(i–iv) shows the TEM images for the vesicles without addition of any drugs. The images were taken with freshly prepared vesicles to avoid any fusion event whose absence is clearly evident in each of the figures. As the DMPE content increases in the DMPC vesicles, the vesicle size increases. The frequency of distribution study based on the TEM slides (at least four slides were used for each sample) is represented in the Figure 3b (i) to (iv). These histogram plots show an increase in average diameter of the vesicles as the DMPE content increases. It is important to note that the average diameter of the DMPC vesicles containing 10 mol % DMPE is similar to the average diameter of pure DMPC SUVs, which is 50–60 nm. A slight increase in the average diameter to 60–70 nm is seen in case of 20 mol % DMPE while almost 2-fold increase in average diameter, which is in between 110 and 120 nm, occurs in DMPC vesicles containing 30 mol % of DMPE.

The presence of DMPE in the DMPC changes the curvature of the SUVs, which in turn changes the size of the vesicles in the state of suspension. The reason for this lies in the fact that DMPE alone forms the lamellar phase and can form SUVs only in the presence of other cylindrical phospholipids like DMPC.[16,42] Despite vesicle formation in mixed bilayers, DMPE preferentially occupies the outer monolayer at low DMPE concentration and in the inner monolayer at high DMPE concentration at neutral pH.[24,43] This is the principal cause for the altered curvature

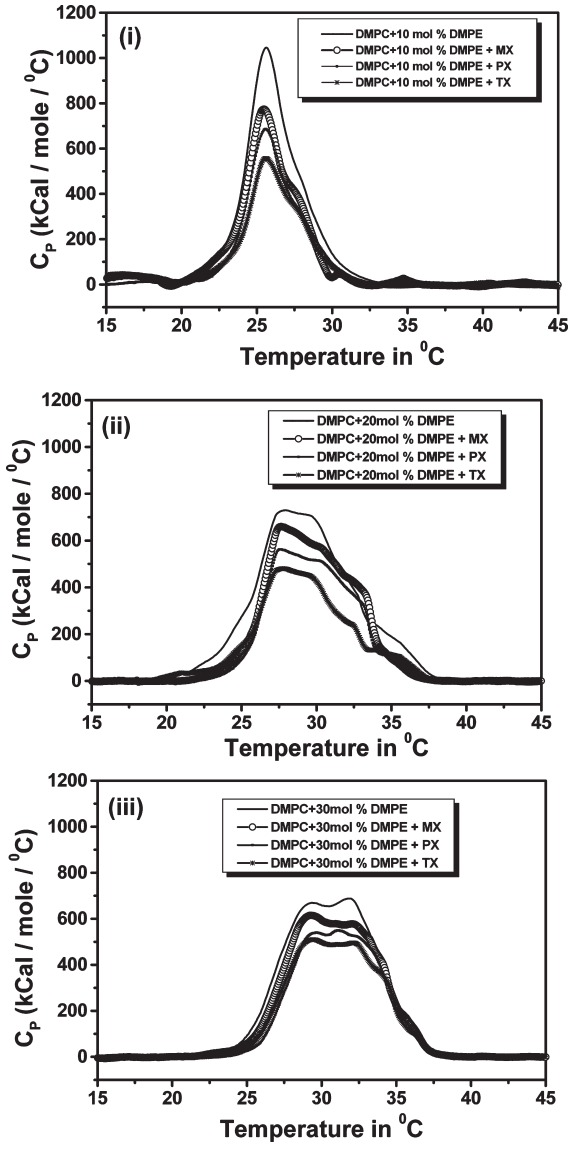

Figure 4. DSC thermograms showing the plot of specific heat (C_P) as a function of temperature for DMPC vesicles containing 10 mol % DMPE (i), 20 mol % DMPE (ii), and 30 mol % DMPE (iii) in the presence of 30 μM of oxicam NSAIDs, namely, Mx, Px, and Tx, for all the cases and at pH 7.4. The scan rates were 20 °C/h for all the experiments.

resulting in an increase in average diameter of the vesicles. Increase in diameter implies reduced curvature. Also larger diameter is detrimental to trans-bilayer movements.[44]

Representative DSC thermograms of 10, 20, and 30 mol % DMPE containing DMPC vesicles treated with 30 μM Mx, Px, and Tx are presented in Figure 4(i−iii). Thermograms of pure DMPC and DMPC containing drugs[12] always show a single main transition. In contrast to pure DMPC vesicles, mixed vesicles in the presence and absence of drugs exhibit heterogeneity in transition temperature accompanied by a broadening. Since there is a wide difference in the gel-to-fluid phase transition temperature (T_M) of the lipids DMPC (24.18 °C)[10] and DMPE (49.7 °C),[21] this broadening is due to typical coexistence of the gel and fluid domains of the lipids, which melt differentially at different temperatures. Temperature dependent atomic force microscopy (AFM) studies of supported DMPC and DMPE mixed bilayers have also clearly shown differential melting of these domains.[15] Addition of the drugs results in a decrease in the transition peak with Tx having the maximum effect followed by Px and Mx. It should be noted that, in all the cases, the gel to sol transition is complete before 39 °C which is our working temperature. The ΔH values increase steadily with the increase in DMPE content in DMPC SUVs. This trend is maintained in the presence of all the drugs but what is interesting is that ΔH values decrease with the increase in hydrophilicity of the drugs used. The ΔH values of the phase changes are tabulated in the Table 2.

Effect on Partition Coefficient (K_P). The effect of a drug on a lipid bilayer is guided by its extent of interaction with the bilayer. This is best expressed by the extent of partitioning of the drugs. Hence, the values of the partition coefficients (K_P) of the oxicam NSAIDs, namely, Mx, Px, and Tx, determined at pH 7.4 and 39 °C in DMPC vesicles containing varying concentrations of DMPE are determined and shown in Figure 5a. The representative plots showing the increase in the fluorescence intensity of the three oxicam drugs with increase in lipid concentration are given in Figure 5b(i−iii) that have lipid compositions of DMPC and 10 mol % of DMPE. Similar kinds of plots as in Figure 5b (i−iii) were obtained for all other lipid compositions and are given in the Supporting Information [Figure S1a(i−iii) and Figure S1b-(i−iii)]. The partition coefficients were calculated from a non-linear fit of the data using eq 1. The values of I_{max} in eq 1 were calculated from the linear plot of eq 2, which are given in the insets of Figure 5b(i−iii). In the case of Figures S1a (i−iii) and S1b(i−iii), the insets contain the respective plots for the determination of the values of I_{max}.

Figure 5a clearly shows that with increasing concentration of DMPE in DMPC vesicles the partitioning of Mx increases significantly. However, the K_P values of Px and Tx decrease with the increase in the mol % of DMPE. The values of K_P at 30 mol % of DMPE show very weak partitioning of Tx inside the vesicles. From Figure 5a, it is evident that the most hydrophobic drug among the three oxicam NSAIDs, that is, Mx [log P (octanol/water) = 0.7], partitioned maximally inside the DMPE containing DMPC SUVs, whereas the most hydrophilic one, that is, Tx [log P (octanol/water) = −0.75] shows minimum partitioning. Px [log P (octanol/water) = −0.14] having intermediate hydrophilic character also shows a decrease in the K_P values with an increase in DMPE concentration in the vesicles which is less pronounced than that in the case of Tx.[10,45] It can therefore be concluded that incorporation of DMPE in DMPC vesicles makes the bilayer more and more hydrophobic. Strong interaction of PE headgroups with neighboring lipids results in the formation of a more closely packed lipid bilayer,[15,23] along with the fact that PE headgroups are associated with fewer water molecules,[46] result in increased hydrophobicity of the mixed bilayers. This allows the lipophilic drug Mx to go deeper inside the bilayer but makes it more difficult for the relatively hydrophilic drugs Px and Tx to partition inside the vesicles.

Effect on Lipid Mixing. The time courses obtained from the lipid mixing assay in the presence of Mx and in the absence of any drug, that is, the control, are represented in Figure 6a(i) and b(i), respectively. The time courses in the presence of the other two drugs, namely, Px and Tx, are given as the Supporting Information Figure S2a(i) and S2b(i), respectively. The extent of lipid mixing in the presence of all the drugs is much larger than in absence of them. The values of rate constants of lipid mixing, calculated from the time courses, are given in Table 1 and plotted

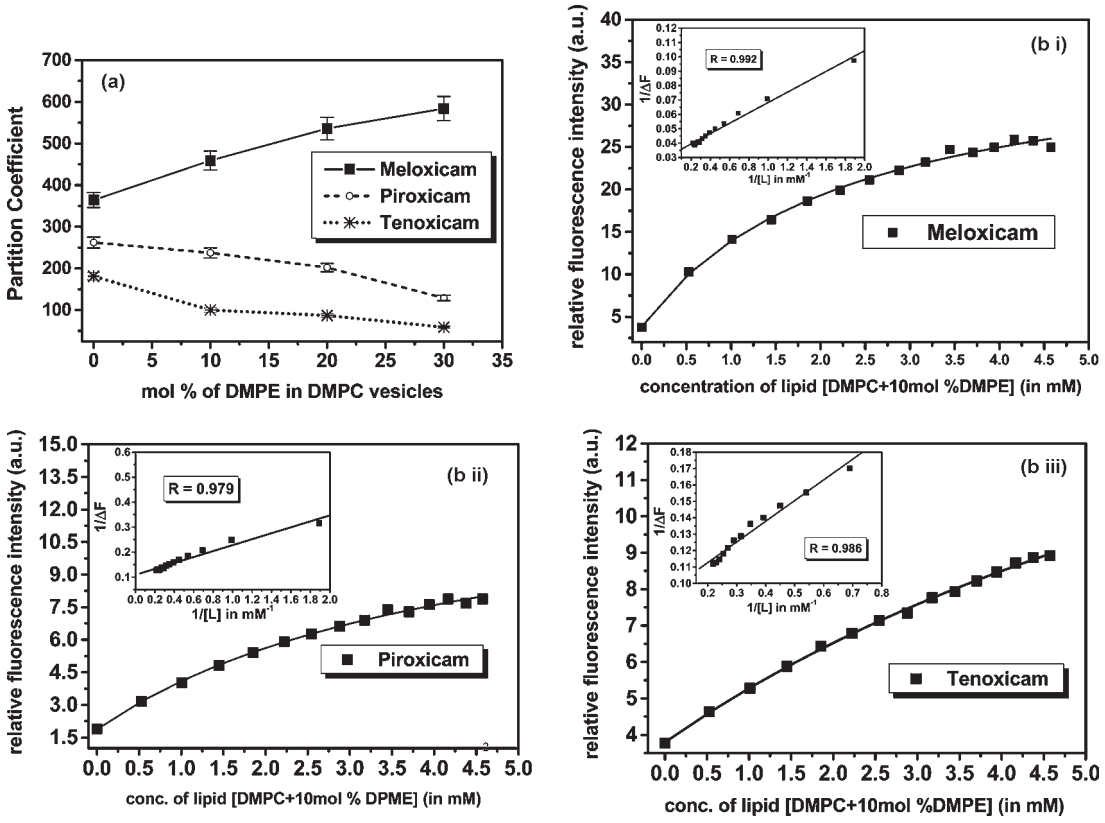

Figure 5. (a) Plot of calculated values of partition coefficient (K_P) of the oxicam NSAIDs, namely, Mx, Px, and Tx, between the DMPC vesicles containing varying concentration of DMPE vs mol % of lipid. The concentration of the drugs remained constant at 30 μM. Other experimental conditions remained the same. (b) Plot of relative fluorescence intensity of Mx (i), Px (ii), and Tx (iii) vs mole concentration of DMPC containing 10 mol % DMPE added. All the drugs used have the concentration of 30 μM, and the temperature and the pH of the experiments were 39 °C and 7.4, respectively. Plots of $1/\Delta F$ vs $1/[L]$ for the respective drugs are plotted and are given in the insets of b(i−iii).

in Figure 7a. The rate constant of lipid mixing for Mx first increases rapidly when 10 mol % DMPE is present in DMPC SUVs but then sharply falls as the DMPE content increases in the vesicles. A similar trend is also found in case of lipid mixing rates, in the presence of the other two drugs and in the absence of any drug, that is, for control. However, only in case of Mx, there is a dramatic increase with subsequent decrease in lipid mixing rates. The values of lipid mixing rates for all the mixed bilayers decrease in the order Mx > Px > Tx. This follows the trend in the extent of partitioning in the bilayer.

In contrast to the lipid mixing rates, there is a continuous increase in the extent of lipid mixing in the presence of increasing DMPE concentration. The extents of lipid mixing in presence of the three drugs at various concentration of DMPE in DMPC SUVs are given in the inset of the Figure 7a. The sharp increase in the extent of lipid mixing in the case of Mx means that the number of vesicles undergoing fusion has increased rapidly. This increase in extent is less pronounced in the presence of Px and Tx.

Effect on Content Mixing and Leakage. The time courses obtained from the content mixing assay and leakage assay in the presence of Mx and in the absence of any drug, that is, the control, are represented in Figure 6a(ii) and b(ii), respectively, for content mixing assay and Figure 6a(iii) and b(iii), respectively, for leakage assay. The time courses of content mixing assay and leakage assay in the presence of the other two drugs, namely, Px and Tx, are given in Supporting Information Figure S2a(ii) and b(ii) for content mixing assay and Figure S2a(iii) and b(iii) for leakage assay, respectively. The values of rate constants of content mixing and leakage, calculated from these time courses, are given in Table 1 and plotted in Figure 7b for content mixing. For all cases, the lipid mixing rates are much faster than the content mixing rates which are consistent with the sequential fusion model as shown by us.[11,12] The rate constants of content mixing for Mx first increase rapidly up to 20 mol % DMPE but then sharply fall as the DMPE content increases to 30 mol %. Such a dramatic change in content mixing rates is not seen in the case of the other two drugs Px and Tx as well as the control. However, a closer look at Table 1 shows a similar trend in all the other cases, namely, Px, Tx, and control, but the changes in values are rather small. The extent of content mixing, as presented in the inset of Figure 7b, shows a mild increase up to 20 mol % DMPE present in DMPC vesicles for Mx and then a sharp increase at 30 mol % DMPE. Such a large increase is not seen in other cases. It should be noted that, for all the drugs including the control, content mixing maximizes at 20 mol % DMPE, which is in contrast to lipid mixing rates that maximize at 10 mol %. The reason for this discrepancy will be explained in the Discussion below. Our leakage data show that leakage is more competitive with content mixing than the preceding lipid mixing events.

4. DISCUSSION

Headgroup size mismatch keeping the lipid tails identical does not simply affect the packing as expected. Several other lipid parameters are also altered. It is known that spontaneous

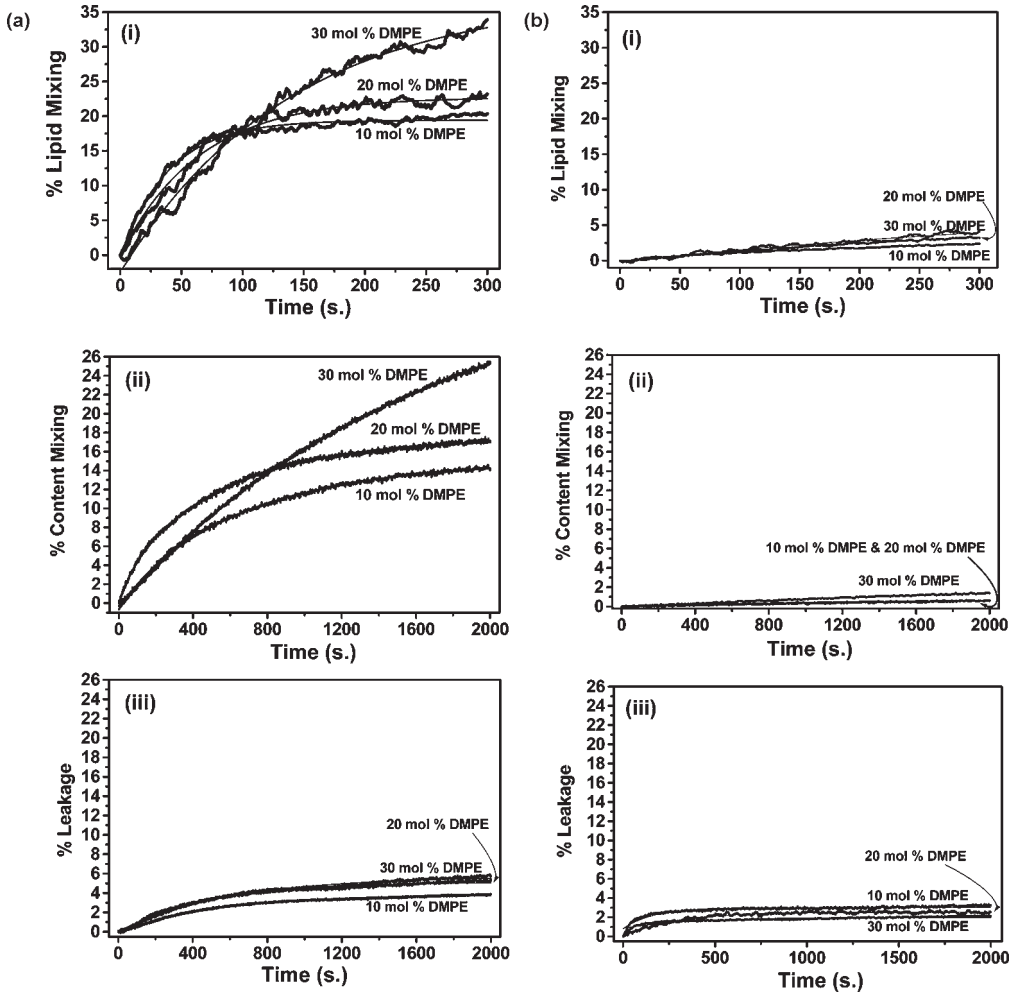

Figure 6. (a) Drug dependent lipid mixing followed by N-NBD-PE/^{N}Rh-PE assay (i); content mixing assay followed by Tb-DPA assay (ii); and leakage followed by Tb-DPA assay (iii) of DMPC vesicles containing DMPE of different concentrations as mentioned with time for 30 μM Mx. The time courses were fit to single exponential curves $[f = a(1 - \exp(-kt))]$ using Origin 7.0. The temperature was kept constant at 39 °C throughout the experiments. (b) Lipid mixing followed by N-NBD-PE/^{N}Rh-PE assay (i); content mixing assay followed by Tb-DPA assay (ii); and leakage followed by Tb-DPA assay (iii) of DMPC vesicles containing DMPE of different concentrations as mentioned with time. In control, no drugs were added; only DMSO having the same volume as the drug was mixed. The time courses were fit to single exponential curves $[f = a(1 - \exp(-kt))]$ using Origin 7.0. The temperature was kept constant at 39 °C throughout the experiments.

trans-bilayer flip-flop movements are strongly affected by the presence of 10−30 mol % DMPE in DMPC vesicles, leading to a decrease in spontaneous fluctuation defects, which in turn are known to decrease fusion.[9] Besides, mismatch in packing between PE and PC headgroups leads to altered curvature, thereby increasing the average diameter of the vesicles as seen from our TEM studies. It should be mentioned that significant changes in average diameter occur only at 20 mol % and it becomes almost double at 30 mol % DMPE. An increase in diameter results in a decrease in vesicle curvature which is known to affect the fusion events adversely.[44] Also, an increase in diameter inhibits trans-bilayer movements whose effect is to decrease fusion synergistically. Another important effect comes from the heterogeneous distribution of DMPC and DMPE. DMPEs are known to occupy the outer monolayer more at a low concentration of DMPE in the SUVs. At higher concentration (30 mol % or more), the distribution of DMPE increases in the inner monolayer as compared to the outer monolayer. Since both DMPE and DMPC have different shapes and form monolayers with different spontaneous curvature, this disparity in DMPE distribution affects the spontaneous curvature of the bilayer.

Heterogeneity and the broadening in the transition temperature as seen in our DSC thermograms is a clear indicator of the presence of coexisting gel and fluid domains. What is interesting is that the presence of the three drugs does not affect the domains but decreases the gel−sol transition temperature enthalpy. In the absence of the drugs, increased ΔH values with increasing DMPE fractions are due to stronger intermolecular attraction particularly between the headgroups. As a consequence of this strong interaction between the headgroups, there is a closer packing of the lipid molecules resulting in a decrease in area occupied per lipid molecule and more aligned tails. This hinders the mobility of the lipid tails as they get less room to move freely. This hindered mobility of the tails is consistent with the fact that there is a reduction in the spontaneous fluctuation defects. Even though the trend remains same for each drug, the ΔH values decrease with the hydrophilicity of the drugs.[45] This could indicate that the gel−sol transition is less inhibited with

dx.doi.org/10.1021/la2030186 |*Langmuir* 2011, 27, 15054–15064

Table 1. Calculated Values of Rate Constants of Lipid Mixing, Content Mixing, and Leakage in the Presence of Oxicam NSAIDs, namely, Mx, Px, and Tx, and in the Absence of Drugs (Control)[a]

DMPC/DMPE	control	meloxicam	piroxicam	tenoxicam
		lipid mixing assay		
100:0	0	$(2.45 \pm 0.04) \times 10^{-3}$	$(7.81 \pm 1.50) \times 10^{-3}$	$(4.60 \pm 0.32) \times 10^{-3}$
90:10	$(4.56 \pm 0.08) \times 10^{-3}$	$(25.17 \pm 0.57) \times 10^{-3}$	$(8.46 \pm 0.85) \times 10^{-3}$	$(6.52 \pm 0.76) \times 10^{-3}$
80:20	$(2.71 \pm 0.03) \times 10^{-3}$	$(15.39 \pm 0.75) \times 10^{-3}$	$(6.15 \pm 0.61) \times 10^{-3}$	$(3.71 \pm 0.09) \times 10^{-3}$
70:30	$(2.22 \pm 0.03) \times 10^{-3}$	$(7.23 \pm 0.45) \times 10^{-3}$	$(5.19 \pm 0.43) \times 10^{-3}$	$(2.36 \pm 0.10) \times 10^{-3}$
		content mixing assay		
100:0	0	$(0.99 \pm 0.12) \times 10^{-3}$	$(0.52 \pm 0.06) \times 10^{-3}$	$(0.42 \pm 0.05) \times 10^{-3}$
90:10	$(0.43 \pm 0.03) \times 10^{-3}$	$(3.63 \pm 0.17) \times 10^{-3}$	$(0.76 \pm 0.04) \times 10^{-3}$	$(0.68 \pm 0.07) \times 10^{-3}$
80:20	$(0.44 \pm 0.04) \times 10^{-3}$	$(7.17 \pm 0.26) \times 10^{-3}$	$(0.86 \pm 0.06) \times 10^{-3}$	$(0.71 \pm 0.05) \times 10^{-3}$
70:30	$(0.23 \pm 0.06) \times 10^{-3}$	$(0.61 \pm 0.05) \times 10^{-3}$	$(0.41 \pm 0.02) \times 10^{-3}$	$(0.28 \pm 0.02) \times 10^{-3}$
		leakage assay		
100:0	0	$(2.95 \pm 0.10) \times 10^{-3}$	$(1.11 \pm 0.40) \times 10^{-3}$	$(1.92 \pm 0.17) \times 10^{-3}$
90:10	$(\mathbf{6.09} \pm 0.15) \times 10^{-3}$	$(1.38 \pm 0.03) \times 10^{-3}$	$(3.68 \pm 0.12) \times 10^{-3}$	$(3.81 \pm 0.25) \times 10^{-3}$
80:20	$(3.59 \pm 0.08) \times 10^{-3}$	$(2.07 \pm 0.03) \times 10^{-3}$	$(6.71 \pm 0.31) \times 10^{-3}$	$(2.34 \pm 0.07) \times 10^{-3}$
70:30	$(2.74 \pm 0.04) \times 10^{-3}$	$(1.69 \pm 0.02) \times 10^{-3}$	$(1.22 \pm 0.05) \times 10^{-3}$	$(1.46 \pm 0.10) \times 10^{-3}$

[a] The concentration of the drugs remained constant at 30 μM, and the temperature and pH were kept at 39 °C and 7.4, respectively, throughout the experiments.

Table 2. Gel to Fluid Phase Transition Enthalpy Values in kJ mol^{-1} of DMPE Containing DMPC Vesicles [DMPE Concentration Varies from 10 mol % to 20 mol % and Finally to 30 mol %] and in the Absence and in the Presence of 30 μM Oxicam NSAIDs As Obtained from the DSC Experiments

	enthalpy of phase transition (kJ mol^{-1})			
DMPC/DMPE	no drug	meloxicam [log P = 0.7][a]	piroxicam [log P = −0.14][a]	tenoxicam [log P = −0.75][a]
100:0	10.24 (±0.41)	7.59 (±0.07)	5.31 (±0.04)	4.60 (±0.06)
90:10	17.66 (±0.13)	12.72 (±0.15)	11.38 (±0.09)	9.83 (±0.04)
80:20	24.14 (±0.45)	19.30 (±0.18)	16.61 (±0.14)	14.71 (±0.15)
70:30	22.34 (±0.34)	19.79 (±0.12)	17.27 (±0.08)	16.46 (±0.4)

[a] The log P (octanol/water) values are taken from the ref 45.

increasing hydrophilicity of the drugs. We have deliberately kept the working temperature at 39 °C where the gel−sol transition is complete.

The extent of interaction of the drugs with these mixed bilayers having altered lipidic parameters is best quantized by their partition coefficients. Our results show that the most hydrophobic drug Mx shows a large increase in partitioning with increasing DMPE, whereas for both Px and Tx the partition coefficient decreases. There are two factors that work together to make the mixed bilayers more hydrophobic. As has been mentioned above, the PE headgroup has a greater ability to interact strongly with neighboring lipid molecules than PC, leading to a close-packed lipid bilayer with aligned hydrocarbon tails. Also, due to the shape and smaller size of the PE headgroups, fewer water molecules are associated with it which makes the PE headgroup more dehydrated compared to PC. These two factors together lead to a more hydrophobic bilayer interior. Mx being the most hydrophobic drug[45] prefers the more hydrophobic bilayer environment as compared to Px and Tx.

Compared to the pure DMPC bilayer, which does not show any fusion under the experimental conditions used, some amount of fusion is seen in the case of DMPC-DMPE mixed vesicles. This is expected since DMPE is known to induce fusion due to its ability to form the inverted hexagonal phase (H_{II}), which in turn creates a negative spontaneous curvature of the bilayer that helps to stabilize the fusion intermediates and hence facilitates fusion.[47] The increase in lipid mixing rates at 10 mol % DMPE in the presence and absence of the drugs is due to the increase in spontaneous fluctuation defects and thereby the increase in flip-flop motion due to the decrease in activation free energy of trans-bilayer motion.[1] Curvature does not play any role at this concentration. TEM studies have indicated identical average diameter compared to that of pure DMPC vesicles. However, this trans-bilayer motion is hindered at 20 and 30 mol % DMPE due to a more close packing of the headgroups, leading to a subsequent decrease in lipid mixing. Moreover a decrease in curvature also acts synergistically to decrease fusion. The rates are maximum for Mx that shows highest partitioning followed by Px and Tx, whose partitioning decreases in that order. As shown by our previous studies,[10,11] higher partitioning promotes fusion.

In contrast to lipid mixing, content mixing rates maximize at 20 mol % DMPE. To elucidate this discrepancy, one needs to revisit the fusion pathway of protein-free lipidic fusion.[9] Two types of intermediates dominate the fusion pathway, namely, hemifusion intermediate state or "stalk" that require extensive lipidic motion for effective mixing and fusion pore opening

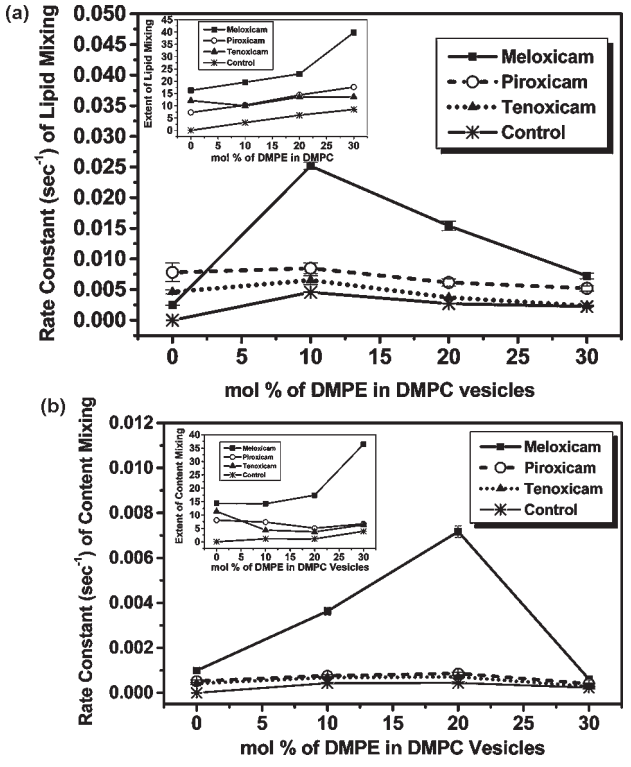

Figure 7. (a) Plot of calculated values of rate constants of lipid mixing of DMPC vesicles containing several concentrations of DMPE, namely, 10, 20, and 30 mol %, in the presence of 30 μM Mx, Px, and Tx vs mol % DMPE at similar experimental conditions. The inset shows a plot of the extent (a) of lipid mixing of DMPC vesicles containing several of concentrations of DMPE, namely, 10, 20, and 30 mol %, in the presence of 30 μM Mx, Px, and Tx vs mol % DMPE present in the mixed vesicles. (b) Plot of calculated values of rate constants of content mixing of DMPC vesicles containing several of concentrations of DMPE, namely, 10, 20, and 30 mol % in the presence of 30 μM Mx, Px, and Tx vs mol % DMPE at similar experimental conditions. The inset shows a plot of the extent (a) of content mixing of DMPC vesicles containing several of concentrations of DMPE, namely, 10, 20, and 30 mol %, in the presence of 30 μM Mx, Px, and Tx vs mol % DMPE present in the mixed vesicles.

leading to content mixing. Hemifusion intermediate involves mixing of the outer leaflet of the opposed membranes without the participation of the inner bilayer. Forming a stable fusion pore leading to content mixing requires the mixing of the inner leaflet of the bilayers.[48] Hemifusion intermediate requires an extensive outer leaflet lipid molecule rearrangement attaining a net negative curvature, whereas the subsequent formation of the fusion pore requires a typical arrangement of the inner monolayer to attain a net positive curvature.[49] It is well established that DMPE has a conelike effective shape and tends to form monolayers with net negative curvature.[48] As mentioned earlier, DMPE occupies mainly the outer leaflet in DMPC-DMPE bilayers at 10 mol % DMPE. At 20 mol % DMPE, its concentration further increases in the outer leaflet, but there is an accompanying decrease in the trans-bilayer movement. The presence of DMPE in the outer leaflet promotes negative curvature due to lipid mixing up to 10 mol % DMPE, leading to an increase in lipid mixing as well as stable hemifusion formation and finally content mixing. Beyond this concentration, the lipid mixing rates decrease due to restricted trans-bilayer motion. On the other hand, stable pore formation leading to content mixing requires positive curvature of the inner leaflet which is promoted by the presence of less DMPE and hence more DMPC in the inner monolayer up to 20 mol % DMPE. Beyond 20 mol %, DMPE starts moving toward the inner monolayer which in turn hinders the positive curvature of the inner layer thereby inhibiting pore formation and content mixing. Moreover, the subsequent decrease in content mixing rates is also due to the decrease in spontaneous fluctuation defects arising from trans-bilayer flip-flop motion and also due to reduction in curvature. Here too the values of the content mixing rates follow the same trend as lipid mixing with Mx > Px > Tx.

To sum up our results, the headgroup mismatches result in altering several lipid parameters which all affect the fusion event. The changes in these lipid parameters and the oxicam NSAIDs work hand in hand to either induce or inhibit the fusion process. The amplification of the effect of NSAIDs on the fusion event at all intermediate states such as lipid mixing and content mixing is directly dependent on the extent of partitioning of the drugs in the bilayer.

■ ASSOCIATED CONTENT

Supporting Information. Additional figures. This material is available free of charge via the Internet at http://pubs.acs.org.

■ AUTHOR INFORMATION

Corresponding Author

*Fax: +91-33-23374637. E-mail: munna.sarkar@saha.ac.in.

■ ACKNOWLEDGMENT

We acknowledge the help of Mr. Pulak Ray and Mr. Ajay Chakrabarti of Biophysics Division of Saha Institute of Nuclear Physics for their help in TEM. We also thank Prof. Dipak Dasgupta of Biophysics Division for useful suggestions during the DSC experiments.

■ REFERENCES

(1) Wimley, W. C.; Thompson, T. E. *Biochemistry* **1991**, *30*, 1702–1709.
(2) Wimley, W. C.; Thompson, T. E. *Biochemistry* **1990**, *29*, 1296–1303.
(3) Papahadjopoulos, D.; Jacobson, K.; Nir, S.; Isac, T. *Biochim. Biophys. Acta* **1973**, *311*, 330–348.
(4) Wong, M.; Thompson, T. E. *Biochemistry* **1982**, *21*, 4126–4132.
(5) Wiedemann, C. Nat. *Rev. Neurosci.* **2009**, *10*, 172.
(6) Stein, K. K.; Primakoff, P.; Myles, D. *J. Cell Sci.* **2004**, *117*, 6269–6274.
(7) Rothman, J. E.; Söllner, T. H. *Science* **1997**, *276*, 1212–1213.
(8) Harrison, S. C. *Nat. Struct. Mol. Biol.* **2008**, *15*, 690–698.
(9) Cevc, G.; Richardsen, H. *Adv. Drug Delivery Rev.* **1999**, *38*, 207–232.
(10) Chakraborty, H.; Mondal, S.; Sarkar, M. *Biophys. Chem.* **2008**, *137*, 28–34.
(11) Mondal, S.; Sarkar, M. *J. Phys. Chem. B* **2009**, *113*, 16323–16331.
(12) Mondal Roy, S.; Bansode, A. S.; Sarkar, M. *Langmuir* **2010**, *26*, 18967–18975.
(13) Chakraborty, H.; Chakraborty, P. K.; Raha, S.; Mandal, P. C.; Sarkar, M. *Biochim. Biophys. Acta, Biomembr.* **2007**, *1768*, 1138–1146.
(14) Chen, E. H.; Olson, E. N. *Science* **2005**, *308*, 369–373.
(15) Nussio, M. R.; Voelcker, N. H.; Sykes, M. J.; McInnes, S. J. P.; Gibson, C. T.; Lowe, R. D.; Miners, J. O.; Shapter, J. G. *Biointerphases* **2008**, *3*, 96–104.
(16) Ishii, F.; Nii, T. *Colloids Surf., B* **2005**, *41*, 257–262.

(17) Nussio, M. R.; Liddell, M.; Sykes, M. J.; Miners, J. O.; Shapter, J. G. *J. Scanning Probe Microsc.* **2007**, *2*, 41–45.
(18) Domenech, O.; Sanz, F.; Montero, M. T.; Harnandez-Borell, J. *Biochim Biophys. Acta* **2006**, *1758*, 213–221.
(19) Chiantia, S.; Ries, J.; Kahya, N.; Schwille, P. *ChemPhysChem* **2006**, *7*, 2409–2418.
(20) Kraft, M. L.; Weber, P. K.; Longo, M. L.; Hutcheon, I. D.; Boxer, S. G. *Science* **2006**, *313*, 1948–1951.
(21) Silvius, J. *Biochim. Biophys. Acta* **1986**, *857*, 217–228.
(22) Leekumjorn, S.; Sum, A. K. *Biophys. J.* **2006**, *90*, 3951–3965.
(23) Kranenburg, M.; Smit, B. *J. Phys. Chem. B* **2005**, *109*, 6553–6563.
(24) Lentz, B. R.; Litman, B. J. *Biochemistry* **1978**, *17*, 5537–5543.
(25) de Vries, A. H.; Mark, A. E.; Marrink, S. J. *J. Phys. Chem. B* **2004**, *108*, 2454–2463.
(26) Chapman, D.; Urbina, J. *J. Biol. Chem.* **1974**, *249*, 2512–2521.
(27) Yeagle, P. L.; Hutton, W. C.; Huang, C.-H.; Martin, R. B. *Biochemistry* **1976**, *15*, 2121–2124.
(28) Sugar, I. P.; Monticelli, G. *Biophys. Chem.* **1983**, *18*, 281–289.
(29) Stillwell, W.; Brengle, B.; Cheng, Y. F.; Wassall, S. R. *Phytochemistry* **1991**, *30*, 3539–3544.
(30) Georgiev, G. A.; Sarker, D. K.; Al-Hanbali, O.; Georgiev, G. D.; Lalchev, Z. *Colloids Surf., B* **2007**, *59*, 184–193.
(31) Huang, C. H. *Biochemistry* **1969**, *8*, 344–352.
(32) Chakraborty, H.; Roy, S.; Sarkar, M. *Chem. Phys. Lipids* **2005**, *138*, 20–28.
(33) Fiske, C. H.; Subbarow, Y. *J. Biol. Chem.* **1925**, *66*, 375–400.
(34) Tsai, R. S.; Carrupt, P. A.; Tayar, N. E.; Giroud, Y.; Andrade, P.; Testa, B. *Helv. Chim. Acta* **1993**, *76*, 842–854.
(35) Banerjee, R.; Chakraborty, H.; Sarkar, M. *Spectrochim. Acta, Part A* **2003**, *59*, 1213–1222.
(36) Santos, N. C.; Prieto, M.; Castanho, M. A. R. B. *Biochim. Biophys. Acta* **2003**, *1612*, 123–135.
(37) Barrantes, F. J.; Antollini, S. S.; Blanton, M. P.; Prieto, M. *J. Biol. Chem.* **2000**, *275*, 37333–37339.
(38) Wang, J. L.; Edelman, G. M. *J. Biol. Chem.* **1971**, *246*, 1185–1191.
(39) Hoekstra, D.; Düzgüneş, N. In *Methods in Enzymology*; Düzgüneş, N., Ed.; Academic Press, Inc.: San Diego, 1993; Vol. 220, pp 15−32.
(40) Düzgüneş, N.; Bagatolli, L. A.; Meers, P.; Oh, Y.-K.; Straubinger, R. M. In *Liposomes: A Practical Approach*, 2nd ed.; Torchilin, V., Weissig, V., Eds.; Oxford University Press: New York, 2003; pp 113−116.
(41) Düzgüneş, N.; Wilschut, J. In *Methods in Enzymology*; Düzgüneş, N., Ed.; Academic Press, Inc.: San Diego, 1993; Vol. 220, pp 3−14.
(42) Sundler, R.; Düzgüneş, N.; Papahadjopoulos, D. *Biochim. Biophys. Acta* **1981**, *649*, 751–758.
(43) Nordlund, J. R.; Schmidt, C. F.; Dicken, S. N.; Thompson, T. E. *Biochemistry* **1981**, *20*, 3237–3241.
(44) Nir, S.; Wilschut, J.; Bentz, J. *Biochim. Biophys. Acta* **1982**, *688*, 275–278.
(45) Luger, P.; Daneck, K.; Engel, W.; Trummlitz, G.; Waguer, K. *Eur. J. Pharm. Sci.* **1996**, *4*, 175–187.
(46) Gruner, S. M.; Cullis, P. R.; Hope, M. J.; Tilcock, C. P. S. *Annu. Rev. Biophys. Biophys. Chem.* **1985**, *14*, 211–238.
(47) Kinnunen, P. K. J. In *Handbook of Nonmedical Applications of Liposomes*; Lasic, D. D., Barenholz, Y., Eds.; CRC Press, Inc.: Boca Raton, FL, 1996, Vol. 1, pp 153−171.
(48) Chernomordik, L. V.; Kozlov, M. M. *Nat. Struct. Mol. Biol.* **2008**, *15*, 675–683.
(49) Chernomordik, L. V.; Chanturiya, A.; Green, J.; Zimmerberg, J. *Biophys. J.* **1995**, *69*, 922–929.